Progress In Electromagnetics Research C, Vol. 137, 169–183, 2023

A Compact Four-Element Modified Annular Ring Antenna for 5G Applications

Chinnathambi Murugan* **and Thandapani Kavitha**

Abstract—The article presents a low-profile quad-port dual-band printed antenna designed for 5G applications. The antenna is printed on a 58.6 mm × 58.6 mm FR4 substrate with a thickness of 0.8 mm. It operates in the 5G spectrum between 3.3 and 3.8 GHz, specifically in the n77 band, with a 10 dB bandwidth impedance. This flexible operating range allows the antenna to cover future frequency bands essential for 5G applications. The design of the antenna focuses on minimizing the distance between antenna components, which results in a significant improvement in isolation performance, greater than 14 dB. This improved isolation allows for a high radiation efficacy of 85% and an overall gain of approximately 4.8 dBi over the operating range. To evaluate the Multiple-Input Multiple-Output (MIMO) performance of the proposed antenna, the researchers developed additional MIMO metrics, including channel capacity, the Envelope Correlation Coefficient (ECC), and Channel Capacity Loss (CCL). These metrics help assess the antenna's ability to handle multiple signals and maintain good performance in MIMO systems. This study shows that the proposed antenna is suitable for a wide range of applications operating over multiple frequency bands. This makes it a promising candidate for 5G applications, as it covers the necessary frequency range and offers good MIMO performance. The antenna's low profile and compact size also make it suitable for various compact and portable 5G devices.

1. INTRODUCTION

The development of technology prepares the way for the technologies of the next generation, which will have considerable needs in terms of both capacity and mobility. This will be the case since the development of technology paves the way. The preparation that is provided by the advancement of technology will make this a possibility in the future. These applications have a need for a wide bandwidth since they have to operate over a number of different frequency bands [1–3]. Cognitive Radio, often known as CR, is an innovative strategy that is presently being developed with the intention of resolving the problem of idle and under used airwaves [4]. This is because a significant chunk of the spectrum is often not used to its full potential. By making use of the spectrum that is currently under utilised by the primary user at that moment, CR is able to increase the efficiency of the spectrum and reduce the danger that it will become crowded [5]. Because of this, it is able to control access to the spectrum in a manner that is not only effective but also efficient for a broad variety of wireless applications. The term "dynamic spectrum management" refers to another name for this method [6]. It is necessary for the antennas that are used in a CR system to be organised in a Multiple-Input Multiple-Output (MIMO) configuration. This is done so that the system's dependability, data rates, and range can all be improved. The use of cognitive radio devices that are underpinned by MIMO [7–9] makes it feasible for users to establish reliable wireless connections with one another. This results in a very high degree

Received 28 June 2023, Accepted 22 August 2023, Scheduled 5 September 2023
* Corresponding author: Chinnathambi Murugan (jaimurugan@gmail.com).
The authors are with the Department of ECE, Vel Tech Rangarajan Dr. Sagunthala R&D Institute of Science and Technology, Avadi, Chennai, Tamilnadu, India.

of efficient use of the spectrum. In addition to this, it guarantees a high quality of service for a large number of different wireless technologies, such as wireless local area networks (WLAN), 5G, and a big number of other wireless technologies [10]. In recent years, there has been a meteoric rise in the number of standards for wireless communication, one of which is the very powerful LTE system [11–18]. The ability to compress an increasing number of functions into a single wireless device is the major driver behind this trend. The other key factor is the miniaturisation of electronic components. Because there is an inverse relationship between the antenna size and the frequency at which it functions, one of the obstacles in the process of designing is to construct a miniature MIMO antenna system that is capable of supporting numerous LTE bands. This is one of the challenges because there is an inverse link between the antenna size and the frequency at which it operates. This is of utmost significance for the lower frequency bands that have a range less than 1 GHz, such as the LTE 700 band. In order to go forward, this is one of the difficulties that has to be conquered first. With the assistance of cognitive radio and MIMO [19–21], the Internet of Things (IoT) has gained popularity due to the vast use it has in a range of sectors, such as the medicine, transportation, transportation, and tracking industries, amongst others. This widespread application has contributed to its rise in popularity. As a direct result of this, the rates of acceptance for technologies such as cognitive radio and multiple-input multiple-output (MIMO) have grown. RFID takes use of very high frequency bands (ranging from 5.72 GHz to 5.87 GHz), very high bandwidths (ranging from 840 MHz to 960 MHz), radio frequency and microwave ranges (ranging from 2.4 GHz to 2.48 GHz), as well as other ranges of frequencies to varying degrees, depending on the application [22]. The range of ultra-high bandwidths starts at 840 MHz and goes up to 960 MHz. An intelligent RFID system should be compatible with a wide range of different wireless protocols, and its antennas should be able to handle several bands and strands of communication simultaneously. These two facets are equally significant portions of the whole. Because engineers have designed several antennas for a wide variety of applications throughout the course of history, the complexity of the communication networks has steadily risen over time. This is a direct cause of the rise in complexity. Because of the miniaturisation of electronics, it is now required to create a large number of very tiny antennas on a very small footprint. This is because footprints are becoming smaller and smaller. This is done to accommodate the requirements of the newly developed technology. Despite their diminutive size, these antennas should provide excellent performance over a wide range of frequency bands [3, 7]. On the other hand, the fact that portable devices have gotten substantially more compact in size has resulted in constraints that are significantly more stringent in terms of both efficacy and bandwidth than they were in the past. There have been a number of distinct creative antenna designs designed for portable devices, and these designs are now available. In particular, more recent editions of the LTE Standards demand that the antenna performs throughout a broad frequency spectrum, which includes as low as 700 MHz to as high as a few gigahertz [10, 13, 21, 22]; this range is referred to as the LTE Frequency Range. The primary challenge is in the design of the antenna, which must take into account both the high frequencies and low frequencies in order to function properly. This is because the antennas have to be larger so as for them to perform efficiently at lower frequencies. Because of this, it is impractical to use these antennas in portable electronics because of their size requirements. Additional difficulties arise when the antenna parts are put on the same substrate. These difficulties include the coupling between two antennas and current localization. This occurs anytime the various parts of the antenna are assembled on a single substrate. When you merge the individual components of the antenna, you are simultaneously confronted with two challenges. It is seen in [11–18] how MIMO antennas may be used with the LTE standard. Because they are compatible with such a wide number of frequencies, these antennas are ideal for the use with a wide variety of technologies, include 4G LTE, GSM 900, WLAN, and others. This makes them very versatile in their use. The use of distributed grounding systems (DGSs) and through holes in the aforementioned antennas have the effect of changing the impedance matching of MIMO antennas, which subsequently in turn has an influence on the performance of the antenna. This is one of the drawbacks associated with the design of antennas in such a manner. To guarantee that there can be as little coupling as is physically feasible, the ground is stretched, and slots are carved into it. This is done in order to meet the requirements. As additional branches and ground extensions are added to the circuit, the complexity of the circuit rises, which also leads to the introduction of parasitic resonances. It was shown in the research publications cited [23–31] that single-input, single-output (SISO) designs had the potential to function as CR antennas. When it is set up in

such a manner, the antenna system will often have both a broadband and a narrowband antenna in its component parts. The degree of complexity that is involved with the design has grown as a direct result of the need of an external tuning circuit in order to tune the narrowband antenna. Because of their close proximity to one another, the numerous components that make up the antenna have a negative impact on the performance of the antenna overall. When it comes to specific types of antenna designs, a stepper motor is essential in order to be able to change the reconfigurable antenna. This makes a significant contribution to the overall cumbersome nature of the system. Additionally, it is unable to detect frequencies that are lower than 1 GHz, thus the detecting range is slightly constrained as a result. This is one of the reasons that the detecting range is somewhat restricted. Because it has the potential to considerably enhance channel capacity, the setup of MIMO CR [32–38] is seeing a considerable surge in demand.

This article focuses on the design and development of a broad-band MIMO antenna for 5G applications. Each radiating component in the MIMO system resonates between 3.3 and 3.8 GHz with significant isolation better than 15 dB. The enhanced isolation offers considerable performance of the proposed antenna system in terms of radiation efficiency, ECC, total active reflection coefficient (TARC), and channel capacity, which results in that the antenna proposed in this research could be a suitable candidate for 5G applications.

The article has been divided into five different parts in order to make it easier to understand the topics that have been suggested for further investigation. The first and second sections focus on an overview of the structure of the MIMO antenna as well as the results that underpin the creation of a design for a single antenna. The surface current distribution and subsequent discussion are covered in Section 3. The investigation of radiation characteristics and MIMO performance are covered under Sections 4 and 5, respectively.

2. ANTENNA DESIGN AND DISCUSSIONS

The construction of the prospective quad-port MIMO antenna is shown in Figure 1(a), along with the particular dimensions of the antenna. All of the proposed MIMO system's antennas have been placed in one of the four corners of an FR4 substrate that is 0.8 mm thick and has a dielectric constant (ξr) of 3.5 and a tangential loss (δ) of 0.02. Because the complete MIMO antenna system is printed orthogonally on a surface measuring 58.6 mm × 58.6 mm, mutual coupling between the antennas is significantly reduced. The total dimensions of a single antenna in the MIMO design are 24 mm × 22.65 mm, which are substantially small for compact 5G devices.

A single antenna in the MIMO system consists of two octagon-shaped circular annular ring of

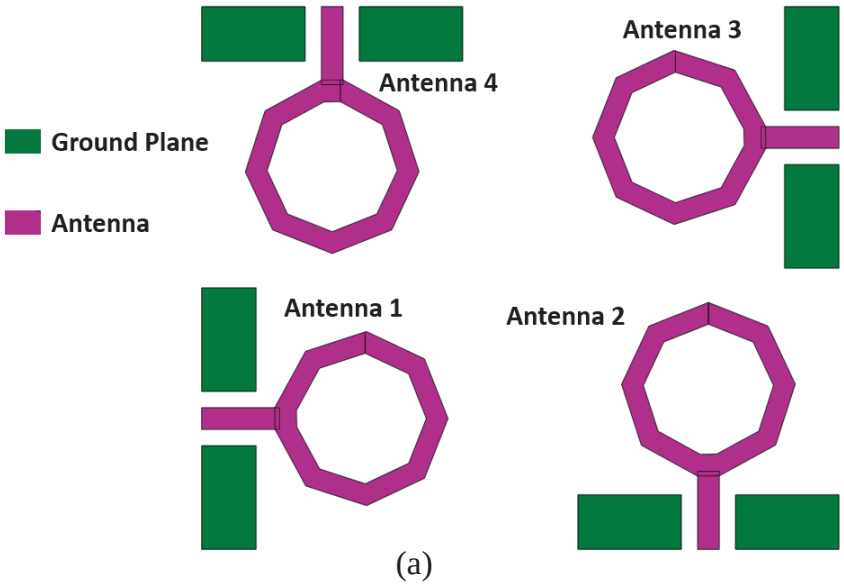

(a)

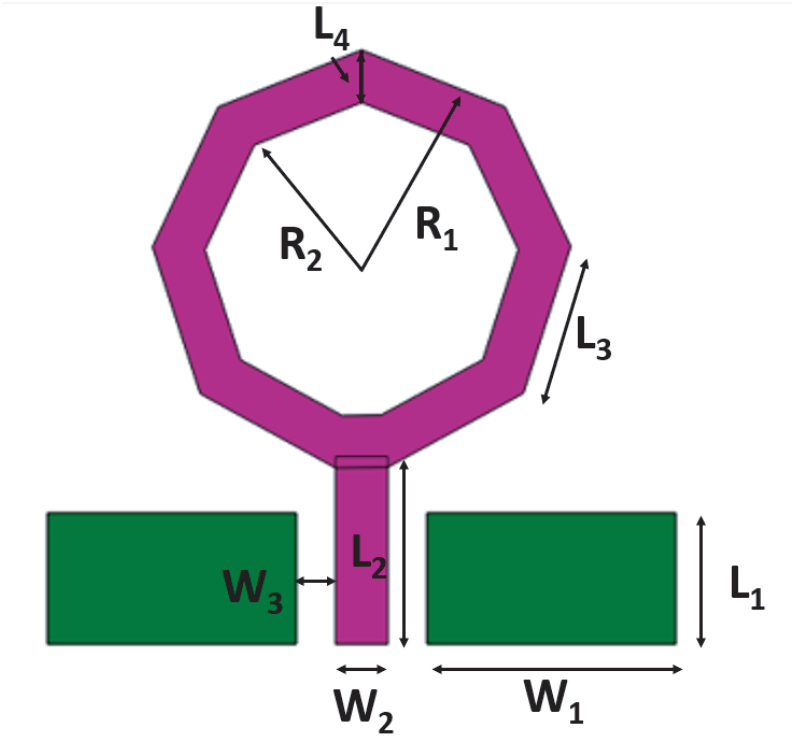

(b)

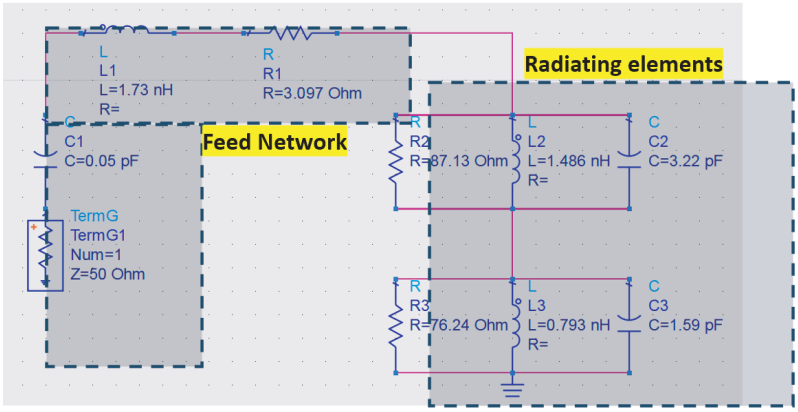

(c)

Figure 1. (a) Overall structure of 4-port MIMO system. (b) Detailed structure of individual antenna. (c) Equivalent circuit of the proposed antenna.

radius $R1 = 7\,\text{mm}$ and $R2 = 6\,\text{mm}$, respectively, and fed by a feeding terminal of dimension $(W2 \times L2)$ $2\,\text{mm} \times 6.75\,\text{mm}$ as shown in Figure 1(b). Then, two rectangular strips of size $(W1 \times L1)$ $9.5\,\text{mm} \times 5\,\text{mm}$ are formed to be a ground plane at front side of the substrate. Figure 1(c) provides equivalent circuit of the proposed antenna and its different passive components values. The equivalent circuit consists of a feeding circuit as well as resonance circuits at the desired band of operation.

3. RESULTS AND DISCUSSIONS

The scattering parameters of a quad-port MIMO antenna are shown in Figures 2(a) and (b). The transmission coefficient and reflection coefficient are two of the scattering parameters that are being

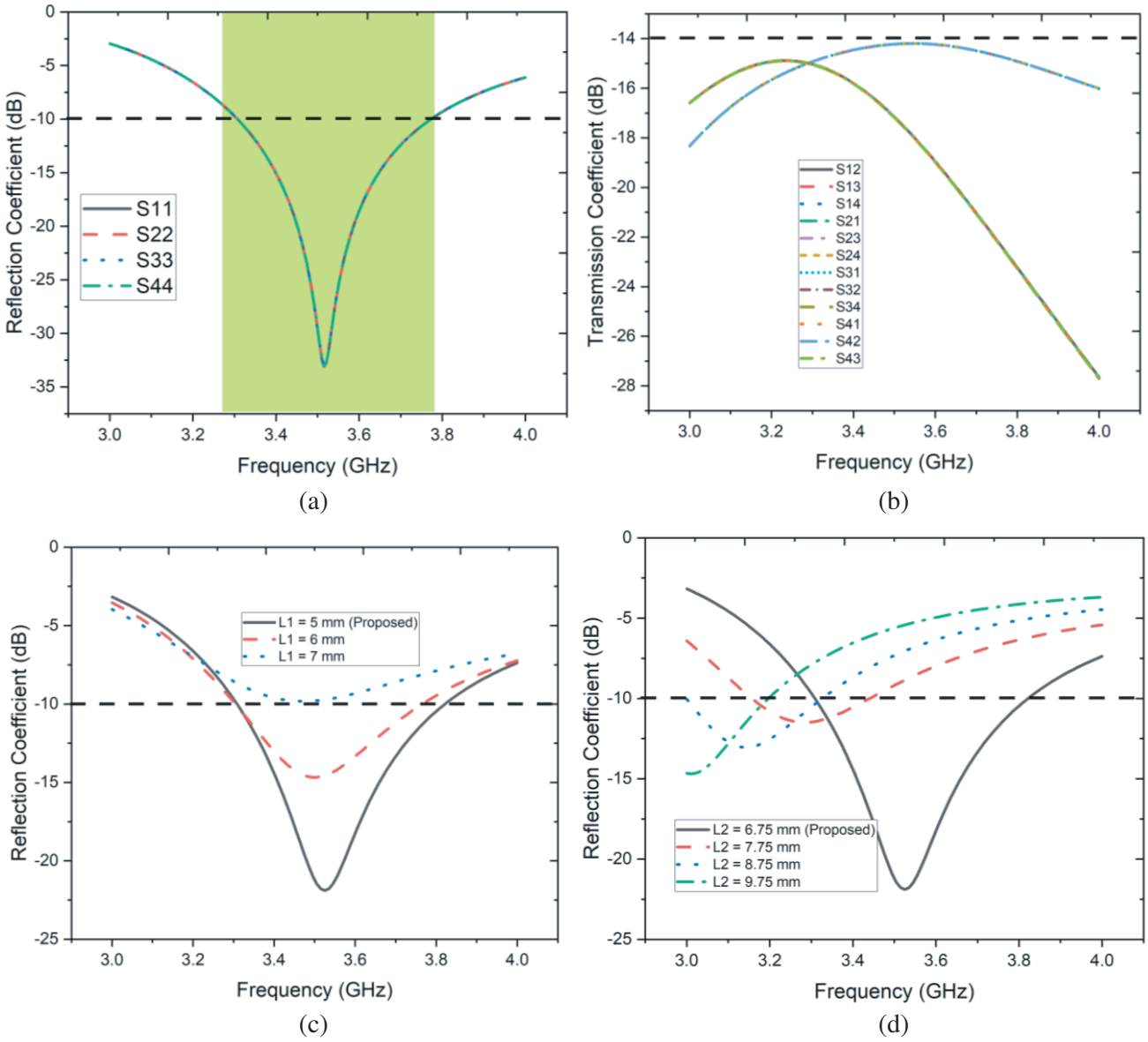

Figure 2. Scattering parameters. (a) Reflection coefficient. (b) Transmission coefficient. **Parametric analysis** when altering (c) $L1$, (d) $L2$.

discussed here. The antenna that has been proposed spans the spectrum from 3.3 to 3.8 GHz throughout the impedance bandwidth of 10 dB, as can be seen in Figure 2(a). The spectrum that is covered accommodates a variety of applications, such as those that use the LTE band 42 (3.4–3.6 GHz) and New radio band 78 (3.3–3.8 GHz) frequencies. In order to demonstrate that the suggested multi-band antenna has appropriate reflection phenomena, all of the occupied spectrum must fall within the bandwidth of 10 dB impedance. Figure 2(b) provides a visual representation of the isolation that exists among the antennas. Over the whole working spectrum, it has been shown that the inter-port isolation among radiating components is greater than 14 decibels. Even after moving antennas such that they are physically closer to one another, a reasonable increase in isolation may still be obtained because of orthogonal configurations. The reflection and transmission coefficients of an antenna are both more than enough for it to function throughout the 5G and WLAN spectrums. The effect of improved isolation is an improvement in the overall performance of the MIMO antenna in regard to MIMO attributes including ECC, TARC, and CCL.

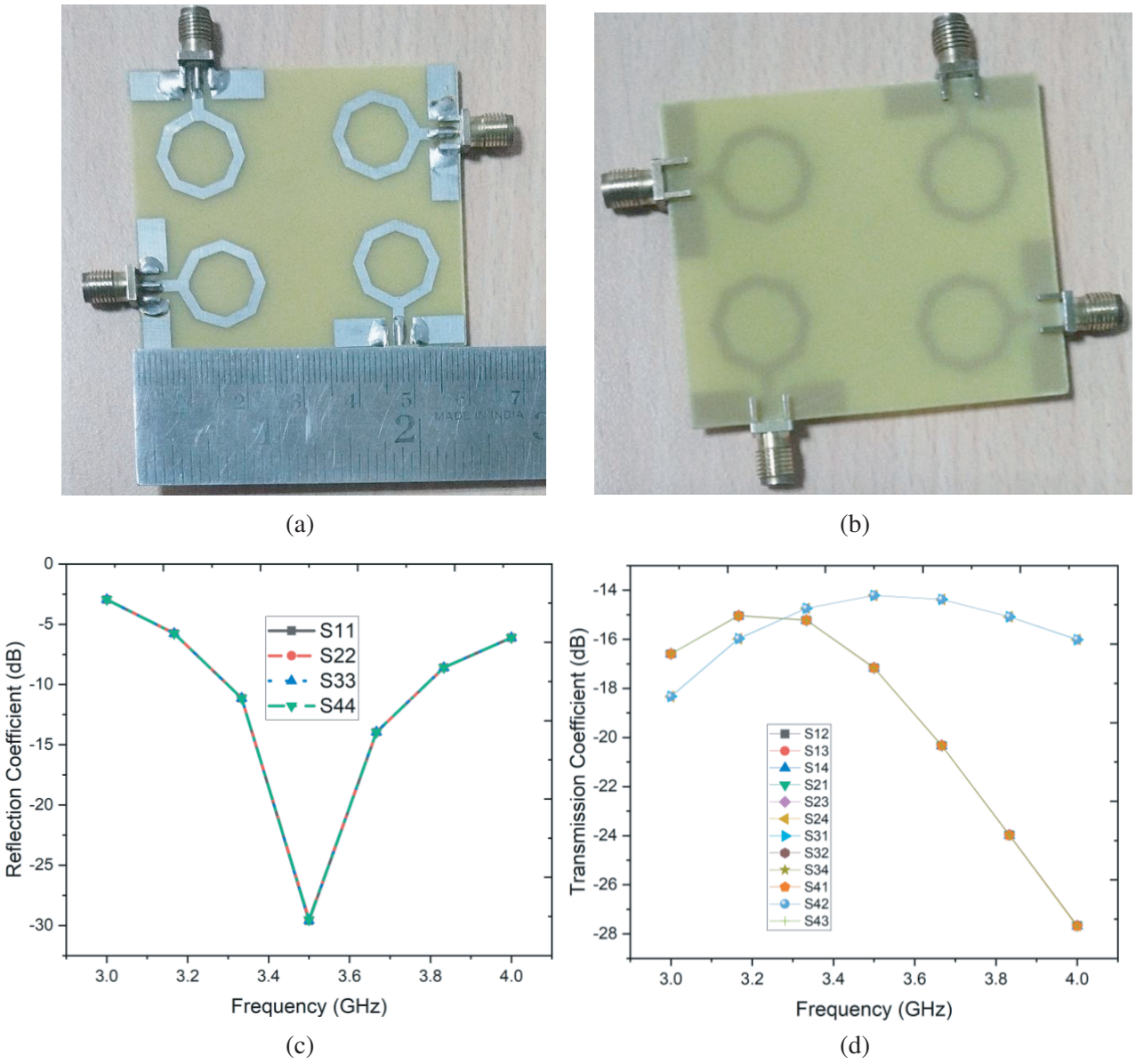

Figure 3. (a) Front and (b) back view of the proposed antenna, measured (c) reflection coefficient, (d) transmission coefficient.

The effects of parameters $L1$ (ground plane length) and $L2$ (length of the feeding terminal) are plotted in Figures 2(c) and (d), respectively. It is observed that $L1$ influences impedance matching of the antenna over the operating spectrum as illustrated in Figure 2(c) whereas $L2$ influences shifting of the operation frequency as shown in Figure 2(d). The prototype of the proposed antenna is illustrated in Figures 3(a) and (b). The measured s-parameters in terms of reflection and transmission coefficients are depicted in Figures 3(c) and (d) respectively, and it is observed that measured outcomes are well matched with simulated results.

4. SURFACE CURRENT DISTRIBUTION

The functioning of the antenna in terms of surface current distribution will be covered in this section. When antenna 1 is stimulated at the desired band of operation (3.4 & 3.8 GHz), the current flow through

antenna 1 does not disrupt the rest of the components due to the orthogonal arrangements of antenna elements as shown in Figures 4(a) & (b). As a result, a reasonable decrease in mutual coupling is accomplished at or above 14 dB. Electric field distribution is provided in Figures 4(c) & (d).

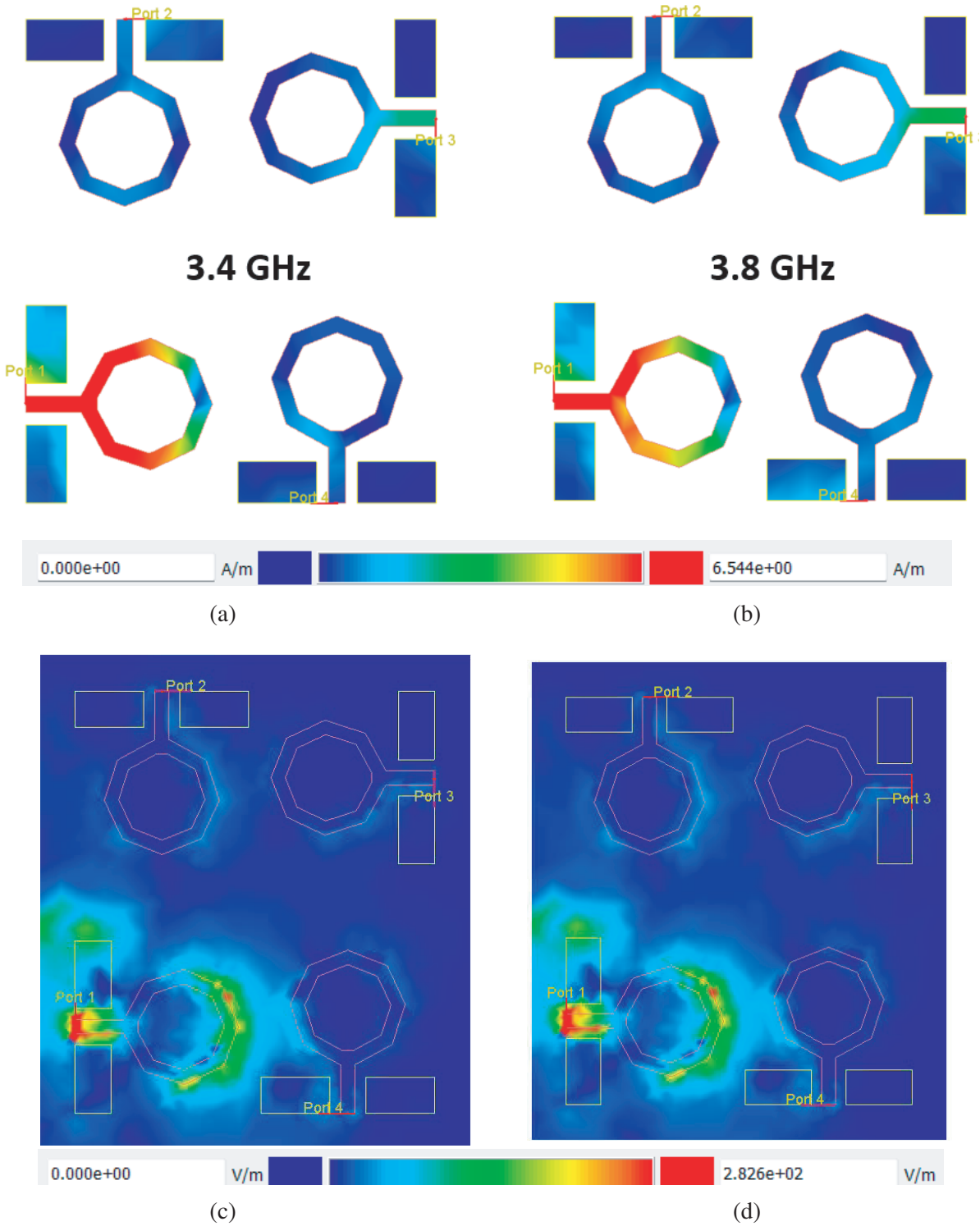

Figure 4. Surface fields of MIMO antenna at (a) 3.4 GHz, (b) 3.7 GHz, *E*-Field distribution (c) 3.4 GHz, (d) 3.7 GHz.

5. RADIATION PERFORMANCE

Figures 5 and 6 show the simulated two-dimensional radiation patterns of an antenna at $O = 0°$ and $90°$ for resonances at 3.4 and 6.5 GHz, respectively. E-Phi (co-polarization) at all frequencies displays enough radiation for both $O = 0°$ and $90°$, as is plainly observable. In contrast, E-theta (cross-polarization) at 3.5 GHz exhibits cross polarization lower than 19 dB, and at 6.5 GHz, it is observed to be 3 dB. The reason for degradation in the cross polarisation between the two resonances of operation is the variation in isolation over the two bands of operation. As discussed earlier, the isolation at low-band (3.4 GHz) is better than 17 dB, which influences cross polarization, causing cross polarization lower than 19 dB. On the other hand, the isolation at higher bands drops to a value of 13 dB, which degrades the performance of an antenna after attaining cross-polarization of 12 dB.

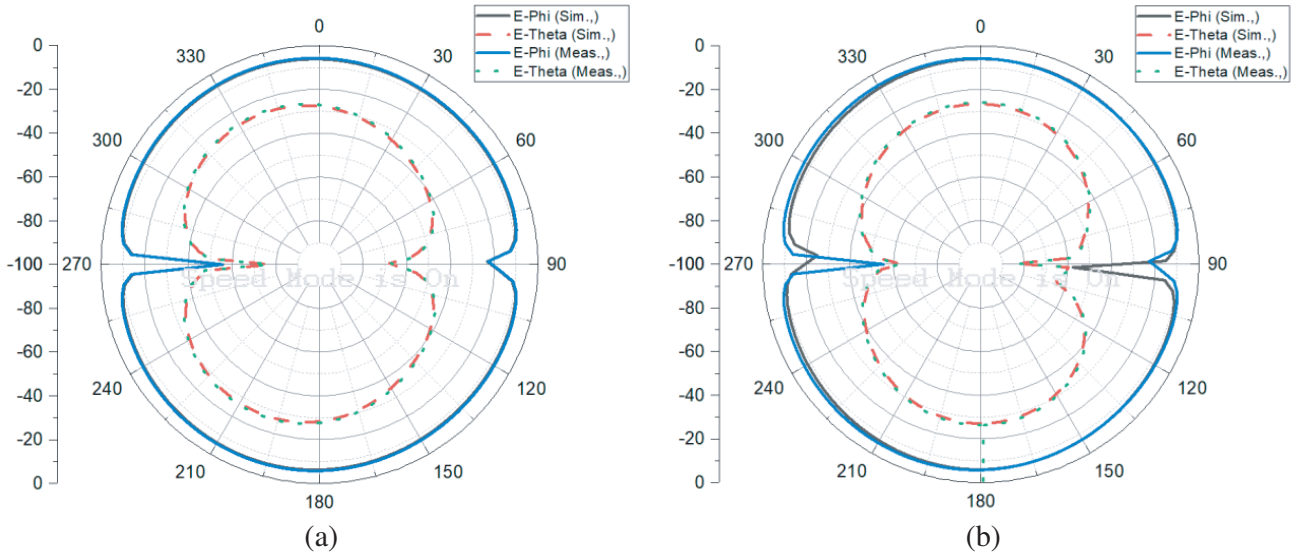

Figure 5. Radiation pattern of antenna 1 at E-Plane. (a) 3.4 GHz, (b) 3.7 GHz.

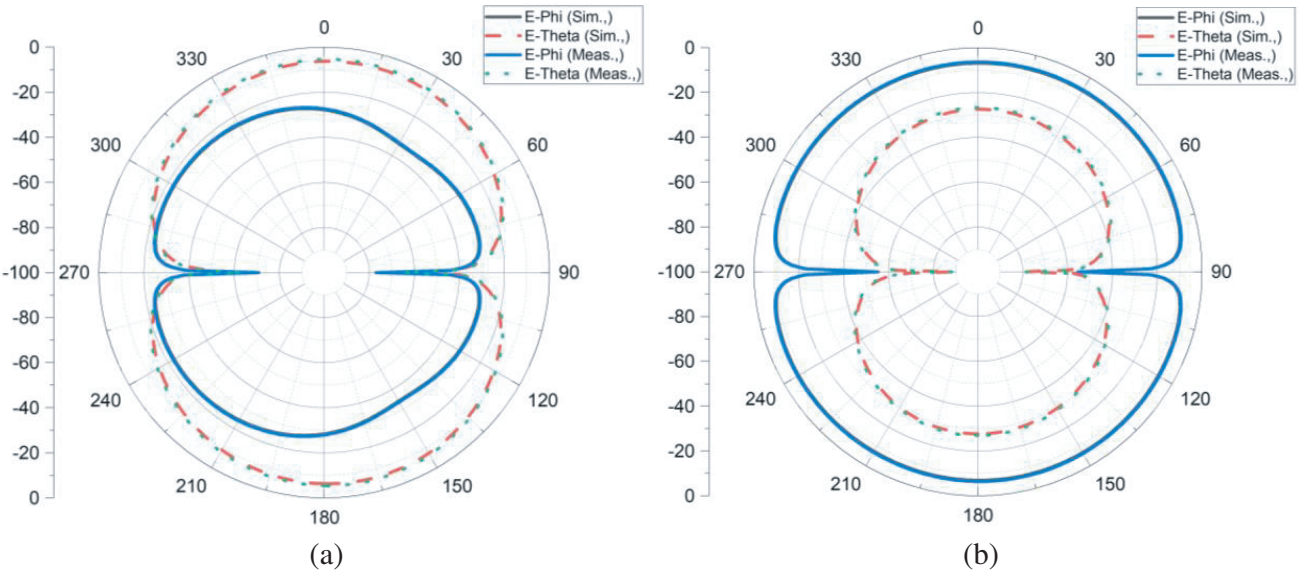

Figure 6. Radiation pattern of antenna 1 at H-Plane. (a) 3.4 GHz, (b) 3.7 GHz.

6. MIMO PERFORMANCE

As is evident from Figure 7(a), all of the estimated ECCs for the various conceivable antenna configurations have values that are lower than 0.1, which means that they satisfy the criteria that are considered acceptable. In light of the fact that a higher diversity gain is accompanied by a lower ECC value, it is possible to draw the conclusion that the proposed quad-port antenna array offers improved diversity performance. Figure 7(b) shows the radiation efficiency of antenna 1 over the dual operating frequencies. It is noticed that the antenna exhibits maximum efficiency up to 90% and 65% from 3.2–3.8 GHz and 5.2–6.86 GHz, respectively. The reason for such degradation in efficiency in the higher band is poor isolation between the elements of the proposed MIMO antenna system. Additionally, we investigate the channel capacity loss of the MIMO antenna, which is more often referred to as CLL. It is able to derive the important data transmission rate feature that is referred to as CLL by using Equation (1) and Equation (2) [47].

$$\text{Channel Loss (CL)} = -\log_2 \det\left(\varphi^R\right) \tag{1}$$

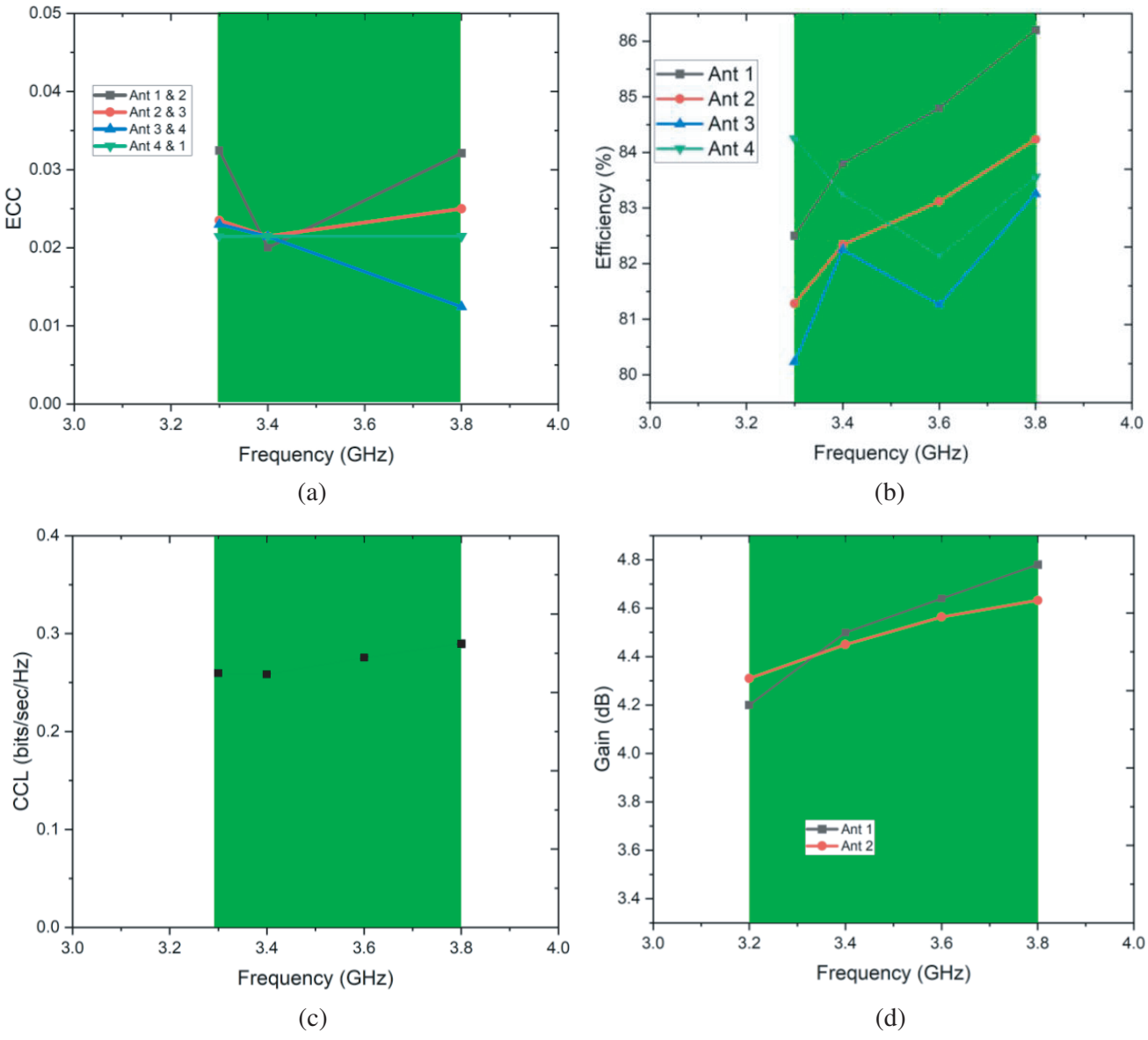

Figure 7. (a) ECC. (b) Efficiency. (c) CCL. (d) Gain.

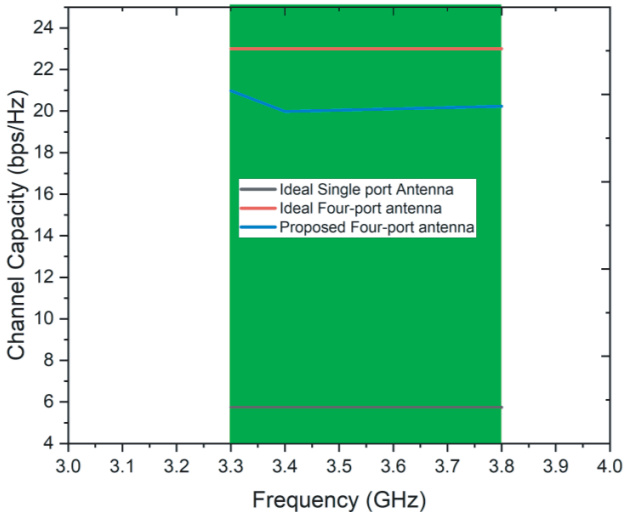

Figure 8. Channel capacity of the proposed antenna.

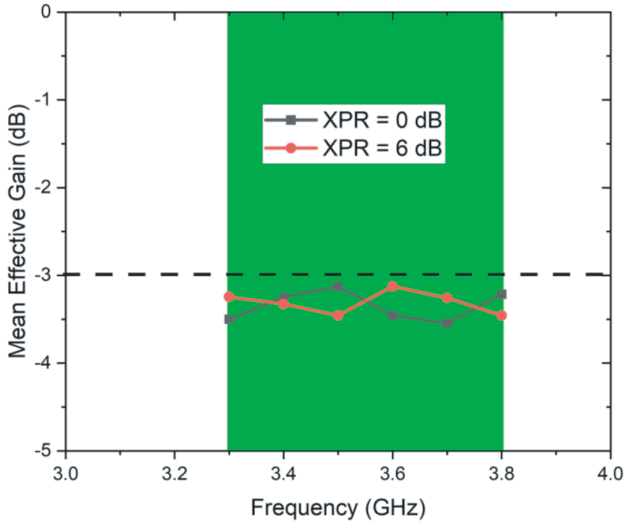

Figure 9. MEG of the proposed antenna.

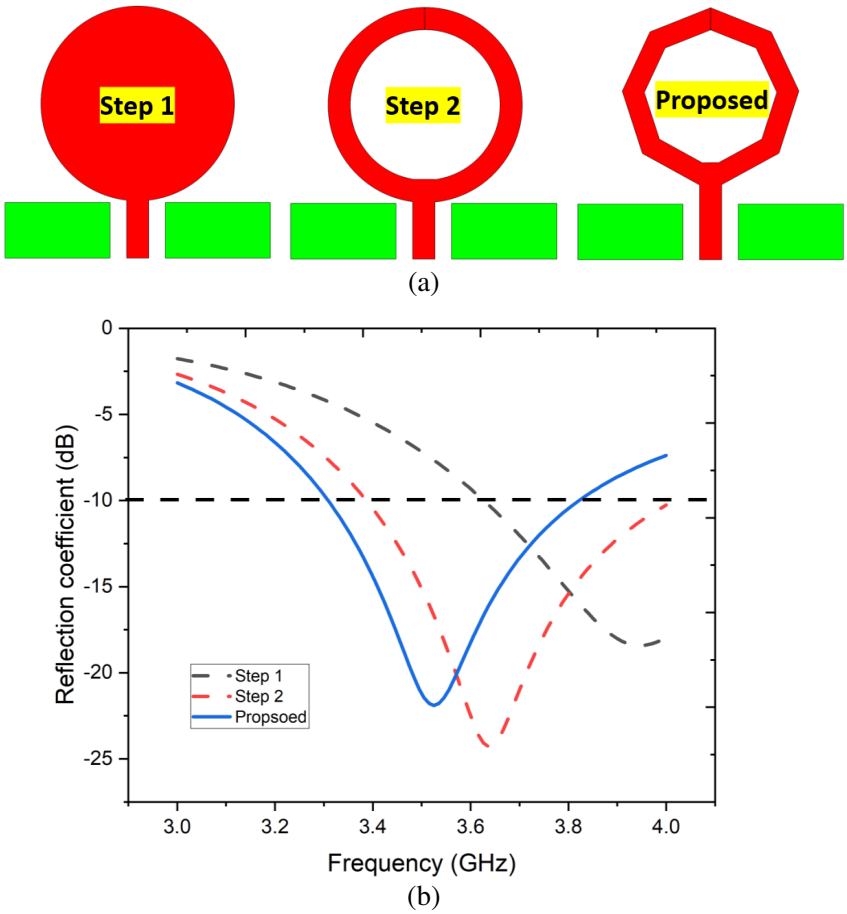

Figure 10. (a) Design evolution of the proposed antenna. (b) Reflection coefficient of the various stages of design evolution.

$$\varphi^R = \begin{bmatrix} ECC_{ii} & \dots & ECC_{ij} \\ \vdots & \ddots & \vdots \\ ECC_{ji} & \dots & ECC_{jj} \end{bmatrix} \tag{2}$$

where,

$$ECC_{ii} = 1 - \left(\left(S_{ii}^2\right) + \left(S_{ij}^2\right)\right)$$
$$ECC_{ij} = -\left(S_{ii}^* S_{ij} + S_{ji}^* S_{jj}\right) \quad for \;\; i,\; j = 1, 2 \dots 4$$

The channel capacity of the designed antenna is estimated to be 21 bps/Hz over the operating spectrum as depicted in Figure 8, and it is found using Equation (3).

$$C = \log\left[\det\left(I + \frac{SNR}{N} H H^T\right)\right] \tag{3}$$

I = Identity matrix, SNR = Signal to Noise Ratio, H = Hermitian matrix, H^T = Hermitian Transpose.

The mean effective gain of the proposed antenna defines how antenna performs, when EM waves propagate in an isometric medium. Figure 9 shows that the proposed antenna exhibits mean effective gain (MEG) lower than 3 dB as required for MIMO antenna system.

$$Mean\ Effective\ Gain\,(MEG) = 0.5\left(1 - \sum_{i=1}^{N} |S_{ij}|\right) \tag{4}$$

The anticipated and reported channel capacity loss brought on by the suggested antenna is seen in Figure 7(c). A CLL value that is acceptable for the full bandwidth is maintained and is less than 0.3

Table 1. Design and performance comparison of the proposed antenna with existing antennas.

Reference No.	**Antenna Structure (mm^3)**	**Frequency of operation (GHz)**	**Dimension of the single antenna (mm^3)**	**Efficiency (%)**	**Gain (dBi)**
[39]	Monopole	0.698–0.96, 1.7–2.7	$65 \times 52 \times 1.6$	NA	1
[40]	Monopole	0.698–0.96, 1.427–2.7	$33 \times 10 \times 55$	> 60	2.8
[41]	Monopole	0.617–0.96, 1.71–5	$60 \times 39.8 \times 15$	> 50	-3
[42]	Monopole	0.917–0.96, 1.71–5,	$60 \times 36 \times 15$	> 45	-2
[43]	Monopole	0.7–0.96, 1.71–6	$84 \times 68 \times 0.17$	NA	3.9
[44]	Monopole	0.72–0.96, 1.6–4	$70 \times 60 \times 1.6$	NA	1.5
[45]	PIFA	0.617–0.96, 1.71–6	$55 \times 50 \times 28$	> 45	-2.5
[46]	Nefer Ant	0.698–6	$80 \times 60 \times 30$	NA	-3
Proposed Work	Defected Ground Structure	3.3–3.8,	$35 \times 30.65 \times 1.6$	> 80	4.8

and 0.39 bits/sec/Hz for low and high bands of resonance. This number assures that the proposed wideband MIMO antenna will achieve adequate data transmission rates and is consistent with the results of CLL simulations. Realized gains of the proposed antennas 1 and 2 are illustrated in Figure 7(d). It is observed that, for low-band, maximum gain is achieved up to 4.8 dB, and for high-band it is obtained up to 4 dB. This is significantly acceptable for 5G antennas.

7. DESIGN EVOLUTION

The stepwise design of the proposed antenna is illustrated in Figure 10(a), and its corresponding performance is depicted in Figure 10(b). It is observed that changes in the structure of the radiating element influence reflection coefficient of the antenna.

The findings of an overview among the results of the proposed antenna as well as that of the existing antennas that were detailed in the earlier research are shown in Table 1. It would seem that the proposed antenna outperforms existing designs with respect to of antenna structure, working frequency, dimensions of the antenna, efficiency, gain, as well as application scope. These factors are all taken into consideration. According to the numerous sources [39–46], it was found that the total dimensions of the individual antenna were significantly smaller than those of the other antennas. This was observed after comparing the overall measurements of the individual antenna to those of the other antennas. The proposed antenna exhibits its superiority by achieving a gain of approximately 4 dB while simultaneously retaining a radiation efficiency of up to 85% across the board for all of the working spectrums. This indicates the antenna's ability to perform over a wide range of frequencies. The findings of this comparison suggest that the antenna that has been described may turn out to be an excellent option for the use in wireless applications that include more than one band.

8. CONCLUSION

The research reveals that a compact quad-port dual-band printed antenna is suitable for 5G applications. The MIMO antenna, which is printed on FR4, measures 58.6 mm × 58.6 mm. The antenna presented in this study is very flexible in its operation, covering the vast majority of currently used and future frequency ranges for 5G applications. The designed antenna maintains a minimal amount of space between its different parts, yet manages to increase isolation performance (by more than 14 dB). This is true whether or not there is physical separation between the antenna's individual parts. These advances in isolation allow antennas to have an overall gain around 4.8 dBi across the appropriate operating band and a radiation efficiency as high as 85%. Because of how thoroughly the area was sealed off, this was finally doable. In order to verify the MIMO performance of the proposed antenna, several MIMO metrics such as ECC, TARC, CCL, and channel capacity have been calculated. Additional research indicates that the given antenna offers sufficient performance for the usage in applications involving many and broad bands.

REFERENCES

1. Shereen, M. K., M. I. Khattak, and J. Nebhen, "A review of achieving frequency reconfiguration through switching in microstrip patch antennas for future 5G applications," *Alexandria Engineering Journal*, Vol. 61, No. 1, 29–40, Jan. 1, 2022.
2. Kim, G. and S. Kim, "Design and analysis of dual polarized broadband microstrip patch antenna for 5G mmWave antenna module on FR4 substrate," *IEEE Access*, Vol. 9, 64306–64316, Apr. 26, 2021.
3. Kumar, G. and K. P. Ray, *Broadband Microstrip Antennas*, Artech House, London, U.K., 2003.
4. Haykin, S., "Cognitive radio: Brain-empowered wireless communications," *IEEE Journal on Selected Areas in Communications*, Vol. 23, No. 2, 201–220, Feb. 7, 2005.
5. Tawk, Y., J. Costantine, and C. Christodoulou, *Antenna Design for Cognitive Radio*, Artech House, Jun. 30, 2016.

6. De Flaviis, F., L. Jofre, J. Romeu, and A. Grau, *Multiantenna Systems for MIMO Communications*, Springer Nature, May 31, 2022.
7. Varzakas, P., "Estimation of radio capacity of a spread spectrum cognitive radio Rayleigh fading system," *Proceedings of the 17th Panhellenic Conference on Informatics*, 63–66, Sep. 19, 2013.
8. Bakulin, M. G., V. B. Kreindelin, and D. Y. Pankratov, "Analysis of the capacity of MIMO channel in fading conditions," *2018 Systems of Signal Synchronization, Generating and Processing in Telecommunications (SYNCHROINFO)*, 1–6, IEEE, Jul. 4, 2018.
9. Chitra, M. P., S. Divya, M. Premkumar, V. Tamilselvi, and N. Karthika, "MIMO cognitive radio capacity in flat fading channel," *2017 Third International Conference on Science Technology Engineering & Management (ICONSTEM)*, 915–919, IEEE, Mar. 23, 2017.
10. Cheng, B. and Z. Du, "Dual polarization MIMO antenna for 5G mobile phone applications," *IEEE Transactions on Antennas and Propagation*, Vol. 69, No. 7, 4160–4165, Dec. 21, 2020.
11. Chen, Y. S. and C. P. Chang, "Design of a four-element multiple-input-multiple-output antenna for compact long-term evolution small-cell base stations," *IET Microwaves, Antennas & Propagation*, Vol. 10, No. 4, 385–392, Mar. 2016.
12. Chen, W. S. and K. H. Lai, "Compact design of MIMO antennas for LTE 700 application," *2015 IEEE International Symposium on Antennas and Propagation & USNC/URSI National Radio Science Meeting*, 1148–1149, IEEE, Jul. 19, 2015.
13. Singh, H. S., G. K. Pandey, P. K. Bharti, and M. K. Meshram, "Compact printed diversity antenna for LTE700/GSM1700/1800/UMTS/Wi-Fi/Bluetooth/LTE2300/2500 applications for slim mobile handsets," *Progress In Electromagnetics Research C*, Vol. 56, 83–91, 2015.
14. Naser, A. A., K. Sayidmarie, and J. S. Aziz, "Compact high isolation meandered-line PIFA antenna for LTE (band-class-13) handset applications," *Progress In Electromagnetics Research C*, Vol. 67, 153–164, 2016.
15. Jan, M. A., D. N. Aloi, and M. S. Sharawi, "A 2×1 compact dual band MIMO antenna system for wireless handheld terminals," *2012 IEEE Radio and Wireless Symposium*, 23–26, IEEE, Jan. 15, 2012.
16. Ikram, M., R. Hussain, A. Ghalib, and M. S. Sharawi, "Compact 4-element MIMO antenna with isolation enhancement for 4G LTE terminals," *2016 IEEE International Symposium on Antennas and Propagation (APSURSI)*, 535–536, IEEE, Jun. 26, 2016.
17. Ikram, M. and M. S. Sharawi, "Compact 10-element monopole based MIMO antenna system for 4G mobile phones," *2016 16th Mediterranean Microwave Symposium (MMS)*, 1–2, IEEE, Nov. 14, 2016.
18. Shoaib, S., I. Shoaib, N. Shoaib, X. Chen, and C. Parini, "Compact and printed MIMO antennas for 2G/3G and 4G — LTE mobile tablets," *2015 IEEE-APS Topical Conference on Antennas and Propagation in Wireless Communications (APWC)*, 674–677, IEEE, Sep. 7, 2015.
19. Li, S., L. D. Xu, and S. Zhao, "The internet of things: A survey," *Information Systems Frontiers*, Vol. 17, 243–259, Apr. 2015.
20. Zaman, M. R., R. Azim, N. Misran, M. F. Asillam, and T. Islam, "Development of a semielliptical partial ground plane antenna for RFID and GSM-900," *International Journal of Antennas and Propagation*, Vol. 2014, Article ID 693412, Jan. 1, 2014.
21. Bukhari, B., C. Singh, K. R. Jha, and S. K. Sharma, "Planar MIMO antennas for IoT and CR applications," *2017 IEEE Applied Electromagnetics Conference (AEMC)*, 1–2, IEEE, Dec. 19, 2017.
22. Bashir, U., K. R. Jha, G. Mishra, G. Singh, and S. K. Sharma, "Octahedron-shaped linearly polarized antenna for multistandard services including RFID and IoT," *IEEE Transactions on Antennas and Propagation*, Vol. 65, No. 7, 3364–3373, May 17, 2017.
23. Ebrahimi, E. and P. S. Hall, "A dual port wide-narrowband antenna for cognitive radio," *2009 3rd European Conference on Antennas and Propagation*, 809–812, IEEE, Mar. 23, 2009.
24. Al-Husseini, M., Y. Tawk, C. G. Christodoulou, K. Y. Kabalan, and A. El Hajj, "A reconfigurable cognitive radio antenna design," *2010 IEEE Antennas and Propagation Society International Symposium*, 1–4, IEEE, Jul. 11, 2010.

25. Tawk, Y., J. Costantine, K. Avery, and C. G. Christodoulou, "Implementation of a cognitive radio front-end using rotatable controlled reconfigurable antennas," *IEEE Transactions on Antennas and Propagation*, Vol. 59, No. 5, 1773–1778, Mar. 3, 2011.
26. Mansoul, A., F. Ghanem, M. R. Hamid, and M. Trabelsi, "A selective frequency-reconfigurable antenna for cognitive radio applications," *IEEE Antennas and Wireless Propagation Letters*, Vol. 13, 515–518, Mar. 11, 2014.
27. Cao, Y., S. W. Cheung, X. L. Sun, and T. I. Yuk, "Frequency-reconfigurable monopole antenna with wide tuning range for cognitive radio," *Microwave and Optical Technology Letters*, Vol. 56, No. 1, 145–152, 2014.
28. Zheng, S. H., X. Y. Liu, and M. M. Tentzeris, "A novel optically controlled reconfigurable antenna for cognitive radio systems," *2014 IEEE Antennas and Propagation Society International Symposium (APSURSI)*, 1246–1247, 2014.
29. Erfani, E., J. Nourinia, C. Ghobadi, M. Niroo-Jazi, and T. A. Denidni, "Design and implementation of an integrated UWB/reconfigurable-slot antenna for cognitive radio applications," *IEEE Antennas and Wireless Propagation Letters*, Vol. 11, 77–80, 2012.
30. Srivastava, G., A. Mohan, and A. Chakrabarty, "Compact reconfigurable UWB slot antenna for cognitive radio applications," *IEEE Antennas and Wireless Propagation Letters*, Vol. 16, 1139–1142, 2016.
31. Nachouane, H., A. Najid, A. Tribak, and F. Riouch, "Dual port antenna combining sensing and communication tasks for cognitive radio," *International Journal of Electronics and Telecommunications*, Vol. 62, No. 2, 121–127, 2016.
32. Hu, Z. H., P. S. Hall, and P. Gardner, "Reconfigurable dipole-chassis antennas for small terminal MIMO applications," *Electronics Letters*, Vol. 47, No. 17, 953–955, 2011.
33. Chacko, B. P., G. Augustin, and T. A. Denidni, "Electronically reconfigurable uniplanar antenna with polarization diversity for cognitive radio applications," *IEEE Antennas and Wireless Propagation Letters*, Vol. 14, 213–216, 2015.
34. Cheng, S. P. and K. H. Lin, "A reconfigurable monopole MIMO antenna with wideband sensing capability for cognitive radio using varactor diodes," *2015 IEEE International Symposium on Antennas and Propagation & USNC/URSI National Radio Science Meeting*, 2233–2234, 2015.
35. Tawk, Y., F. Ayoub, C. G. Christodoulou, and J. Costantine, "A MIMO cognitive radio antenna system," *2013 IEEE Antennas and Propagation Society International Symposium (APSURSI)*, 572–573, 2013.
36. Hussain, R. and M. S. Sharawi, "Integrated reconfigurable multiple-input-multiple-output antenna system with an ultra-wideband sensing antenna for cognitive radio platforms," *IET Microwaves, Antennas & Propagation*, Vol. 9, No. 9, 940–947, 2015.
37. Truncated Cube — From Wolfram MathWorld 2017, http://mathworld.wolfram.com/TruncatedTetrahedron.html, Accessed Dec. 11, 2021.
38. Jha, K. R. and S. K. Sharma, "Combination of frequency agile and quasi-elliptical planar monopole antennas in MIMO implementations for handheld devices," *IEEE Antennas Propagation Mag.*, Vol. 60, 118–131, 2018.
39. Preradov, D. and D. N. Aloi, "Cross polarized 2×2 LTE MIMO system for automotive shark fin application," *Applied Computational Electromagnetics Society*, Vol. 35, No. 10, 1207–1216, 2020.
40. Goncharova, I. and S. Lindenmeier, "A high efficient automotive roof-antenna concept for LTE, DAB-L, GNSS and SDARS with low mutual coupling," *Proceedings of the 2015 9th European Conference on Antennas and Propagation, EuCAP*, 1–5, Lisbon, Portugal, Apr. 2015.
41. Khalifa, M. O., A. M. Yacoub, and D. N. Aloi, "A multiwideband compact antenna design for vehicular sub-6 GHz 5G wireless systems," *IEEE Transactions on Antennas and Propagation*, Vol. 69, No. 12, 8136–8142, Dec. 2021.
42. Yacoub, M., M. O. Khalifa, and D. N. Aloi, "Design of multi-wideband Automotive cell antenna for LTE and 5G applications," *2021 15th European Conference on Antennas and Propagation, EuCAP*, 2021.

43. Sanz-Izquierdo, B., S. Jun, J. Heirons, and N. Acharya, "Inkjet printer and folded LTE antenna for vehicular application," *Proceedings of the 2016 46th European Microwave Conference (EuMC)*, 88–91, London, UK, Oct. 2016.
44. Cheng, Y., J. Lu, and C. Wang, "Design of a multiple band vehicle-mounted antenna," *International Journal of Antennas and Propagation*, Vol. 2019, Article ID 6098014, 11 pages, 2019.
45. Preradov, D. and D. N. Aloi, "Cross polarized 2×2 LTE MIMO system for automotive shark fin application," *Applied Computational Electromagnetics Society*, Vol. 35, No. 10, 1207–1216, 2020.
46. Hastürkoglu, S. and S. Lindenmeier, "A wideband automotive antenna for actual and future mobile communication 5G/LTE/WLAN with low profile," *Proceedings of the 2017 11th European Conference on Antennas and Propagation, EUCAP*, 602–605, Paris, France, Mar. 2017.
47. Iqbal, A., O. A. Saraereh, A. Bouazizi, and A. Basir, "Metamaterial-based highly isolated MIMO antenna for portable wireless applications," *Electronics*, Vol. 7, No. 10, 267, Oct. 22, 2018.